J Mater Sci (2007) 42:4513–4520
DOI 10.1007/s10853-006-0480-2

Cyclic indentation in aluminum

Fuqian Yang · Lingling Peng · Kenji Okazaki

Received: 4 December 2005 / Accepted: 31 May 2006 / Published online: 15 February 2007

Abstract Cyclic indentation was used to evaluate the dynamic deformation of aluminum. Under the load-controlled cyclic indentation, the indenter continuously penetrated into the material and reached a steady state at which the penetration speed (per cycle) was a constant. The amplitude of the cyclic indentation depth was basically controlled by the amplitude of the cyclic indentation load, independent of the mean indentation load and the indentation frequency. The steady state penetration speed decreased with increasing the amplitude of the cyclic indentation load due to the increase in the size of plastic zone. It also decreased with the increase in the mean indentation load due to local strain hardening, while it increased with the increase of the indentation frequency.

Introduction

One of important characteristics in plastic deformation of metallic materials subjected to cyclic mechanical loading is the change of the deformation resistance with the loading cycles. Most metallic materials display the dependence of hardening and/or softening on the loading cycles. Such a change in the deformation resistance is related to the nucleation and propagation of dislocations and to the initiation and accumulation of structural damage, which could eventually lead to the degradation of performance of structural elements in mechanical structures and devices. Several techniques have been developed to evaluate the deformation resistance of materials under the action of cyclic loading, while most of them focus on the global/average response of bulk materials to simple mechanical loading such as uniaxial stresses with relatively small stress gradient [1]. In practical, materials are subjected to multi-axial and non-homogeneous stresses, and the change of the deformation resistance generally originates from local weak areas such as grain boundary and second-phase particles [1, 2]. In general, the deterioration in the deformation resistance is associated with the evolution of localized plastic deformation under the action of dynamic loading. Thus, it is essential to evaluate the local deformation behavior of materials subjected to cyclic mechanical loading.

The depth-sensing indentation technique [3, 4] has been used to characterize the near-surface micromechanical properties of thin films as well as bulk materials, in which the resistance to the penetration of indenter is related to both the elastic and plastic deformation of materials. Based on the indentation technique, cyclic indentation has been performed in the past using the Vickers indenter [5–7], soft metallic cone indenter [8, 9], spherical wolfram carbide indenter [10–14], and steel cylindrical indenter of flat-end [15, 16]. Most of the study focused on the evaluation of the damage zone and on the reduction of strength as a function of the number of indentation cycles. Li and Chu [15] used a flat-ended cylindrical indenter to evaluate the cyclic indentation of β-tin. They observed that the indenter continuously penetrated into the material at a steady state speed (per

F. Yang (✉) · L. Peng · K. Okazaki
Department of Chemical and Materials Engineering, University of Kentucky, Lexington, KY 40506, USA
e-mail: fyang0@engr.uky.edu

cycle). They suggested that the unloading part of a loading-unloading cycle may cause dislocations to be retracted into the source or the shielding effect likely exerts a negative stress concentration at the tip of a sharp (conical or pyramid) indenter or the edge of a cylindrical indenter, so that negative dislocations may be emitted during unloading [15]. In the next loading part of the loading cycle, the renewed stress concentration can cause the emission of more dislocations to propagate the plastic zone.

In general, the cyclic indentation can be either controlled by load or by displacement. For the load-controlled cyclic indentation, a prescribed cyclic indentation load is applied to the indenter. The indentation depth is monitored as a function of time and loading conditions, and the dynamic behavior of materials is evaluated through the change of the indentation depth. For the displacement-controlled cyclic indentation, a prescribed cyclic indentation depth is applied to the indenter. The indentation load is measured as a function of time, and the dynamic deformation of materials is characterized through the change of the indentation load with the indentation depth.

In this work, the load-controlled cyclic indentation of aluminum has been undertaken to evaluate the nature of the mechanical deformation of Al under the action of cyclic indentation. This work focuses on demonstrating the dependence of dynamic deformation of Al on the loading conditions, including the dependence of the steady state penetration speed (per cycle) on the loading amplitude, the mean load of the cyclic loading, and the loading frequency. The cyclic indentation is carried out using a flat-ended cylindrical indenter. The topic is of importance because of current interest in using dynamic indentation to characterize the deformation behavior of materials.

Materials and experimental procedures

The experiments were conducted over the aluminum disks (99+%) purchased from Alfa Aesar, MA. As-received aluminum rod (12 mm in diameter) was machined into a disk shape with diameter of 8 mm and length of 8 mm. The machined Al disks were ground and polished mechanically to obtain two parallel surfaces. The samples then were annealed in furnace at 773 K for 12 h and with furnace cooling to room temperature in order to remove residual stresses generated during machining, grinding and polishing processes. The grain size of the annealed Al was 100 microns observed by using optical microscope.

The load-controlled cyclic indentation tests were performed on a Micro-Combi Tester (CSM Instruments, Needham, MA) at ambient temperature. Figure 1 shows the schematic of the cyclic indentation testing. A flat-ended cylindrical indenter of 0.5 mm diameter was made of tool steel (H-13). Before fully applying the indentation load to the predetermined level, a pre-indentation load of 5 mN was applied to the indenter to maintain full contact between the indenter and the surface of the sample. This avoided the effect of impact loading at the start of a cyclic indentation. Constant indentation loading and unloading speeds were employed, as shown in Fig. 2. The cyclic indentation load at the n-th loading and unloading cycle can be expressed as

$$F = \begin{cases} (F_{\mathrm{m}} - \Delta F) + 4f\Delta F(t - nt_{\mathrm{loading}}) \\ (F_{\mathrm{m}} + \Delta F) - 4f\Delta F[t - (nt_{\mathrm{loading}} + t_{\mathrm{unloading}})] \end{cases} \text{for} \begin{matrix} nt_{\mathrm{loading}} < t < nt_{\mathrm{loading}} + t_{\mathrm{unloading}} \\ nt_{\mathrm{loading}} + t_{\mathrm{unloading}} < t < (n+1)t_{\mathrm{loading}} \end{matrix} \quad (1)$$

where F is the indentation load, F_{m} is the mean indentation load, ΔF is the amplitude of the indentation load, t_{loading} is the starting time for the loading phase, $t_{\mathrm{unloadind}}$ is the starting time for the unloading phase, n corresponds to the n-th loading and unloading cycle, and $f(= 1/2(t_{\mathrm{unloading}} - t_{\mathrm{loading}})$ is the frequency of the cyclic indentation load. The behavior of the cyclic indentation of aluminum was characterized as functions of the mean load, amplitude and frequency.

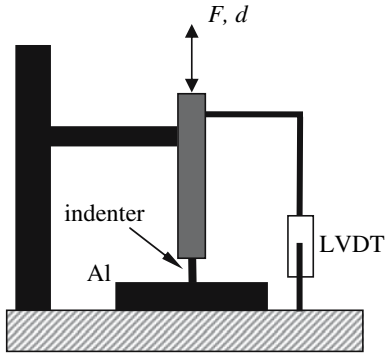

Fig. 1 Schematic of the cyclic indentation test of Al

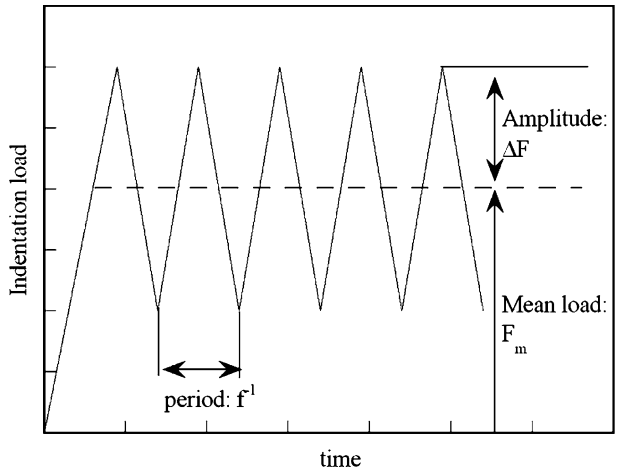

Fig. 2 Schematic of a cyclic indentation load

Results and discussion

Indentation fatigue curves

During the cyclic indentation test, a cyclic indentation load was applied to the indenter, which caused the indenter to move into the surface of the specimen. Both the loading and unloading speeds were maintained constant. The penetration depth of the indentation as a function of time is depicted in Fig. 3 for several indentation loads with different loading amplitudes (the mean load was 700 mN, and the loading frequency was 0.5 cycle per second). After initial offset in the indentation depth due to elastoplastic deformation, the indenter experienced cyclic up-down motion corresponding to the loading-unloading cycle. Under the cyclic loading, the indenter continued to move into the material similar to the creep deformation of materials at elevated temperatures. However different from the creep flow, this is likely related to the dynamic behavior of materials. Negative dislocations are emitted from the sources during the unloading, while more dislocations are emitted in the loading phase. This causes the propagation of the plastic zone underneath the indenter and the propagation of plastic wave. The cyclic indentation produces a steady state speed (per cycle) of the penetration after the transient stage.

It should be pointed out that, for small amplitude of the indentation load, shakedown phenomenon might occur. The cyclic indentation then is controlled by the elastic deformation, and no dislocation is emitted from the edge of the contact zone during the loading-unloading cycle. For large amplitude of the indentation load, dislocations are emitted from the edge of the contact zone. The indenter continuously moves into the material similar to the propagation of cracks under the cyclic loading. The dynamic deformation is controlled by plastic deformation or the emission of dislocations. When the net number of dislocations emitted is nil in each loading-unloading cycle, the dynamic deformation reaches the ratcheting state.

From Fig. 3, it is found that the indentation depth as a function of time can be expressed approximately by the following equation,

$$\delta(t) = \delta_0 + \tilde{\delta}(t) + \Delta\delta \sin(\omega t) \tag{2}$$

where δ_0 is the static indentation depth due to the mean indentation load, $\tilde{\delta}(t)$ represents the change of the average indentation depth in each indentation cycle, and $\Delta\delta$ represents the amplitude of the cyclic indentation depth. In the quasi-steady state of the cyclic indentation, $\tilde{\delta}(t)$ is a linear function of the indentation time.

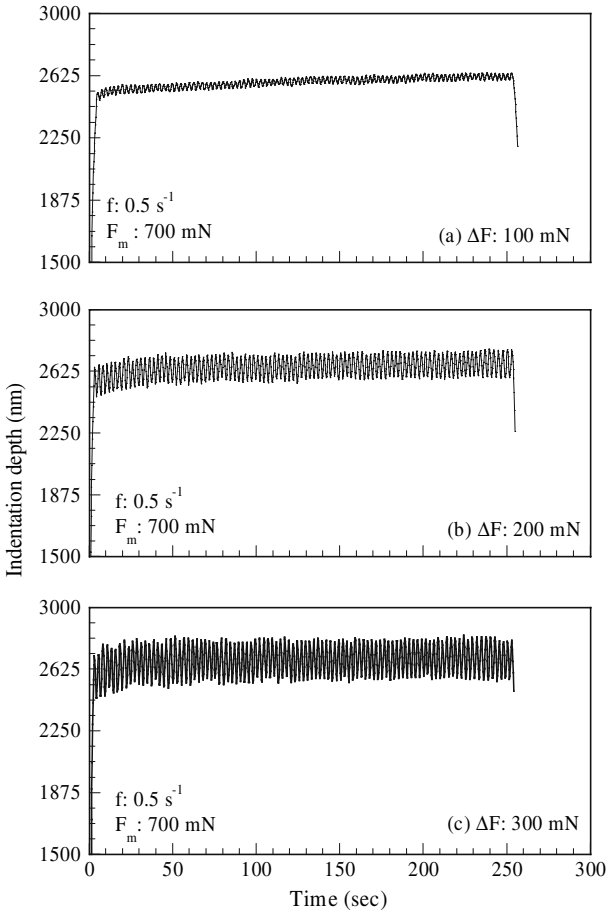

Fig. 3 Indentation depth as a function of time for an indentation load with the mean load of 700 mN and the indentation frequency of 0.5 cycle per second-likely associated with the emission of dislocations from the edge of the contact zone

Effect of the amplitude of the cyclic indentation load

The effect of the amplitude of the cyclic indentation load (ΔF) on the amplitude of the cyclic indentation depth in the steady state indentation is depicted in Fig. 4 for the cyclic indentation loads with the mean indentation load of 700 mN and the indentation frequency of 0.5 cycle per second. The amplitude of the cyclic indentation depth increases with ΔF, as expected. Extending the relation between the indentation load and the indentation depth for the elastic recovery in the quasi-static indentation test to the cyclic indentation, one can have

$$\Delta F = K(\Delta\delta)^{n_1} \tag{3}$$

where K is a constant related to the elastic constants of the specimen and the compliance of the system and n_1 is an index. From Fig. 4, one obtains the index of 0.72.

It is known that, in the quasi-static indentation test the unloading phase is controlled by elastic recovery and the index of n_1 is normally in the range of 1–2 [17]. For the indentation of linear elastic materials using a non-adhesive, rigid, cylindrical flat-ended indenter, Sneddon [18] gave the linear relationship between the indentation load and the indentation depth. Thus, the dynamic deformation of Al during the unloading involves both the elastic recovery and the plastic recovery. As suggested by Li and Chu [15], negative dislocations are likely emitted from the contact edge between the indenter and the specimen, which reduce the dislocation density underneath the indenter and cause local softening and reverse plastic flow. This leads to faster recovery during the unloading and smaller value of the index n_1, compared to the quasi-static indentation.

Figure 5 shows the dependence of the steady state penetration speed $(\mathrm{d}\tilde{\delta}(t)/\mathrm{d}t)$ on the amplitude of the cyclic indentation load. Following the approach in the analysis of the growth behavior of fatigue crack [19], the dependence of the steady state penetration speed on the amplitude of the cyclic indentation load can be expressed as a power law relation

$$\mathrm{d}\tilde{\delta}(t)/\mathrm{d}t = C_1(\Delta F)^{n_2} \tag{4}$$

where C_1 is a constant related to the elastic constants of the specimen and the compliance of the system and n_2 is an index. From Fig. 5, one obtains the index of –1.16. The steady state penetration speed decreases with the increase of the amplitude, which is consistent with the decrease of work hardening rate with the increase of tensile stress in uniaxial tensile test. Higher peak indentation load ($F_m + \Delta F$) creates higher dislocation density underneath the indenter and larger size of plastic zone, which increases the indentation load required to move the indenter further into the material – a decrease in the penetration speed. In other words, at lower amplitude of the cyclic indentation load lower dislocation density is generated compared to that at higher amplitude where dislocations interact with each other to quickly work-harden the material. The steady state penetration speed resembles a plastic strain rate, which strongly depends on the load amplitude.

During each loading-unloading cycle, the dissipation of energy occurs due to the interaction between dislocations and the propagation of the plastic zone.

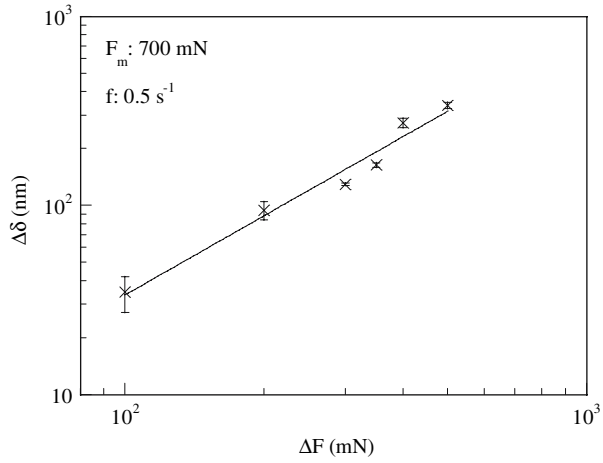

Fig. 4 Dependence of the amplitude of the indentation depth on the amplitude (ΔF) of the cyclic indentation load in the steady state indentation

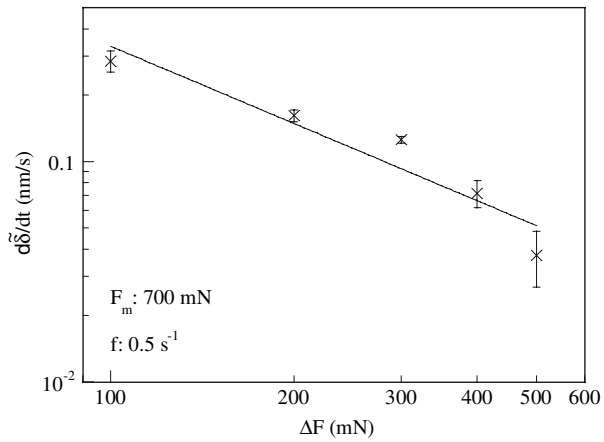

Fig. 5 Dependence of the steady state penetration speed on the amplitude (ΔF) of the cyclic indentation load

The plastic energy dissipated in each loading-unloading cycle, E_{plastic}, can be calculated as

$$E_{\text{plastic}} = E_{\text{loading}} - E_{\text{unloading}} = \oint_{\text{loading}} F\mathrm{d}\delta - \oint_{\text{unloading}} F\mathrm{d}\delta \tag{5}$$

which is the area enclosed by the loading-unloading curve. Figure 6 shows the loading-unloading curves typically at 1, 10 and 100 cycles for the cyclic indentation under the action of a cyclic indentation load with the mean indentation load of 700 mN, load amplitude of 100 mN and indentation frequency of 0.5 cycle/s. Stable hysteresis loops of the indentation load-indentation depth are observed, which resemble those in conventional fatigue tests. The plastic energy dissipated in each cycle appears to be approximately constant, i.e.,

$$E^1_{\text{plastic}} \approx E^2_{\text{plastic}} \approx \cdots\cdots \approx E^{100}_{\text{plastic}} \tag{6}$$

Accordingly, the average plastic energy dissipated per cycle in the cyclic indentation can be calculated as

$$\bar{E}_{\text{plastic}} = \frac{1}{n_{\max}} \sum_{n=1}^{n_{\max}} E^n_{\text{plastic}} \tag{7}$$

where $n_{\max}$ is the maximum indentation cycle carried out in the cyclic indentation test. Figure 7 shows the dependence of the average plastic energy dissipated per cycle on the load amplitude for an indentation load with the mean indentation load of 700 mN and the indentation frequency of 0.5 cycle/s. The average plastic energy dissipated per cycle increases with the increase in the load amplitude as expected.

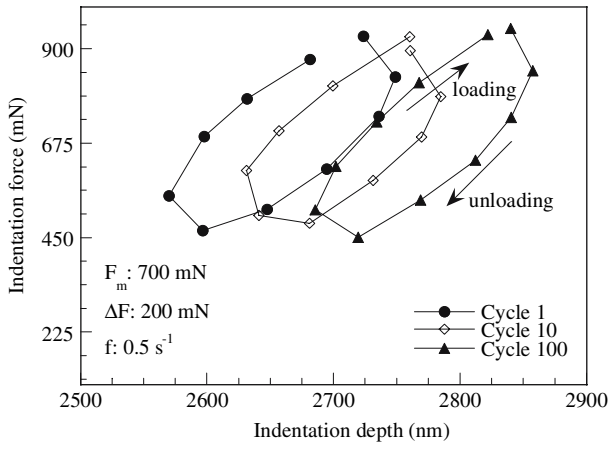

Fig. 6 Loading-unloading curves at the indentation cycle 1, cycle 10 and cycle 100 for an indentation test with the mean load of 700 mN, the load amplitude of 200 mN, and the loading frequency of 0.5 cycle/s

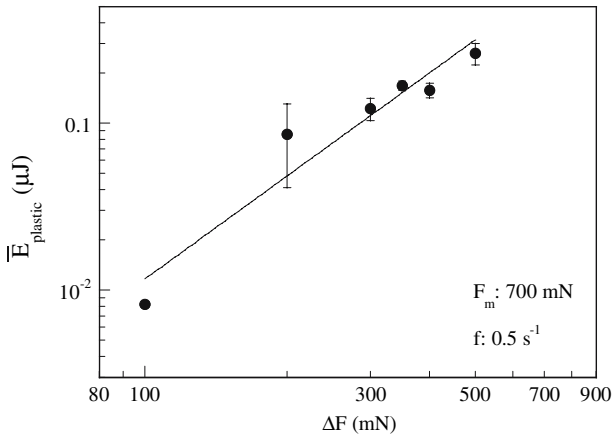

Fig. 7 Dependence of the average plastic energy dissipated per cycle on the amplitude (ΔF) of the cyclic indentation load

Using the similarity analysis, Cheng and Cheng [20] found that the plastic energy dissipated in quasi-static indentations using sharp indenter of geometrical similarity is proportional to the 3/2 power of the indentation load. Yang et al. [21] derived the similar relation by using the dislocation mechanics and the cavity model. It is expected that similar formulae can be used to describe the relation between the average plastic energy dissipated per cycle and the load amplitude of the cyclic indentation load as

$$\bar{E}_{\text{plastic}} = \alpha_1 (\Delta F)^{n_3} \tag{8}$$

where α_1 is a constant and n_3 is an index. From Fig. 7, one obtains n_3 of 2.0, which is different from 3/2 for the quasi-static indentation of Al [21]. This is likely due to the contribution of plastic recovery during the unloading and the work-hardening in the loading cycle to the dynamic plastic deformation of Al. Higher dislocation density is formed underneath the indentation, which requires higher load to cause the motion of dislocations and to induce the propagation of the plastic zone.

Effect of the mean indentation load

In general, the plastic deformation of a material is a function of mechanical loading. To evaluate the effect of the mean indentation load on the cyclic indentation behavior of Al, cyclic indentation loads with the amplitude of the indentation load of 100 mN and the indentation frequency of 0.5 cycle per second were used in the tests. Figure 8 shows the dependence of the amplitude of the cyclic indentation depth in the steady

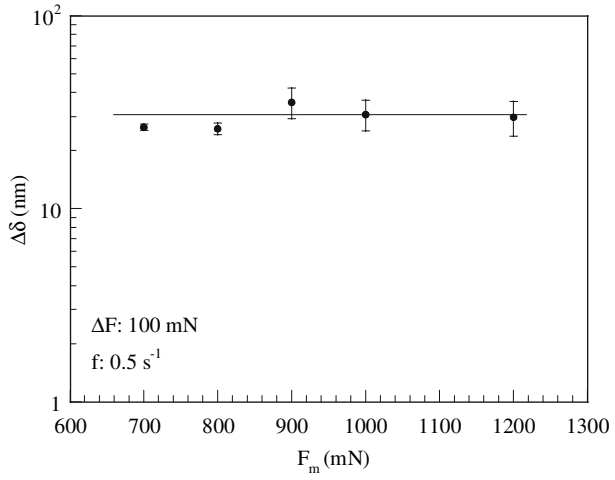

Fig. 8 Dependence of the amplitude of the indentation depth on the mean indentation load for the load amplitude of 100 mN and the load frequency of 0.5 cycle/s

state on the mean indentation load. The amplitude of the indentation depth does not change too much with increasing the mean load, suggesting that the amplitude of the indentation depth is likely controlled by the amplitude of the indentation load as shown in the previous section.

The effect of the mean indentation load on the steady penetration speed is depicted in Fig. 9. The steady state penetration speed decreases with increasing the mean indentation load. It is known that both the size of the plastic zone and the dislocation density underneath the indentation increases with the indentation load in quasi-static indentation [21–23]. Thus it is expected that higher mean indentation load creates larger plastic zone and higher dislocation density. Higher dislocation density promotes strong interaction between dislocations and increases the resistance to the penetration of the indenter, which reduces the penetration speed. This reflects the importance of the mean indentation load in the control of the cyclic indentation. Assuming that the relationship between the steady state penetration speed and the mean indentation load follows a simple power rule as

$$\mathrm{d}\tilde{\delta}(t)/\mathrm{d}t = C_2 F_{\mathrm{m}}^{n_4} \tag{9}$$

where C_2 is a constant and n_4 is an index, one obtains n_4 of –2.4. It should be pointed out that the stress state in the cyclic indentation is much more complicated involving both tensile stress and compressive stress around the contact zone, even though Eq. (9) is similar to the relation between the crack growth rate and the applied stress in describing the propagation of fatigue crack.

Figure 10 shows that the dependence of the average plastic energy dissipated per cycle on the mean load of the cyclic indentation load. Contrary to the dependence of the average plastic energy dissipated per cycle on the load amplitude, the average plastic energy dissipated per cycle decreases with increasing mean load. This is consistent with the observation in the quasi-static indentation of severely deformed Al [24]—less energy is dissipated for severely deformed Al due to higher dislocation density compared to less deformed Al. The strong interaction between dislocations reduces the amount of plastic deformation created by the cyclic indentation and accordingly lowers the energy dissipated in each indentation cycle.

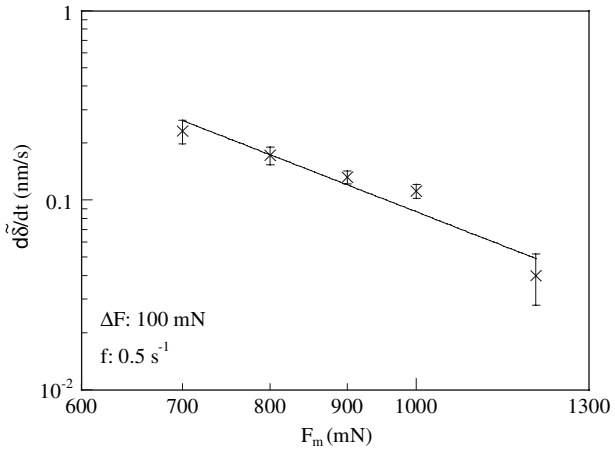

Fig. 9 Dependence of the steady state penetration speed on the mean indentation load for the load amplitude of 100 mN and the load frequency of 0.5 cycle/s

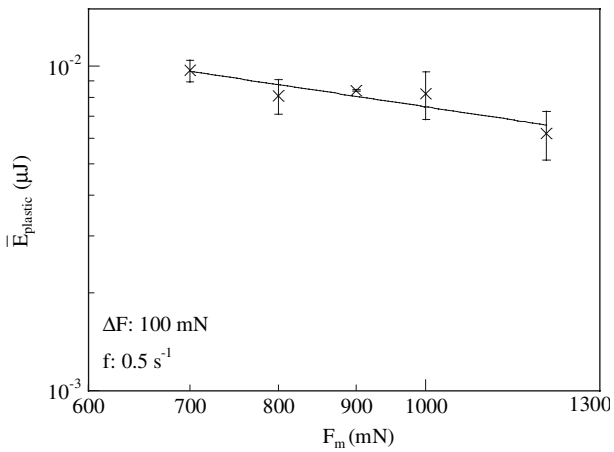

Fig. 10 Dependence of the average plastic energy dissipated per cycle on the mean indentation load for the load amplitude of 100 mN and the load frequency of 0.5 cycle/s

From Fig. 10, one can assume a power law relation between the average plastic energy dissipated per cycle and the mean load of the cyclic indentation load as

$$\bar{E}_{\text{plastic}} = \alpha_2 F_{\text{m}}^{n_5} \tag{10}$$

where α_2 is a constant and n_5 is an index. Using the data as shown in Fig. 10, one obtains n_5 of –5.2.

Effect of the indentation frequency

The dependence of the amplitude of the cyclic indentation depth on the indentation frequency is depicted in Fig. 11. The amplitude of the cyclic indentation depth is independent of the indentation frequency. The results together with those from the previous sections suggest that the amplitude of the cyclic indentation load basically controls the magnitude of the cyclic indentation depth under the current loading conditions, even though both the elastic recovery and the plastic recovery contribute to the deformation during the unloading.

Figure 12 shows the dependence of the steady state penetration speed on the indentation frequency. The steady state penetration speed increases with the indentation frequency. For given mean indentation load and amplitude of a cyclic indentation load, higher indentation frequency increases the speed of dislocation motion, which likely results in quick emission of negative dislocations and faster interaction between dislocations. This reduces the dislocation density directly underneath the indenter and leads to strain-softening. Such strain-softening allows the indenter to move into Al at higher penetration speed. Following

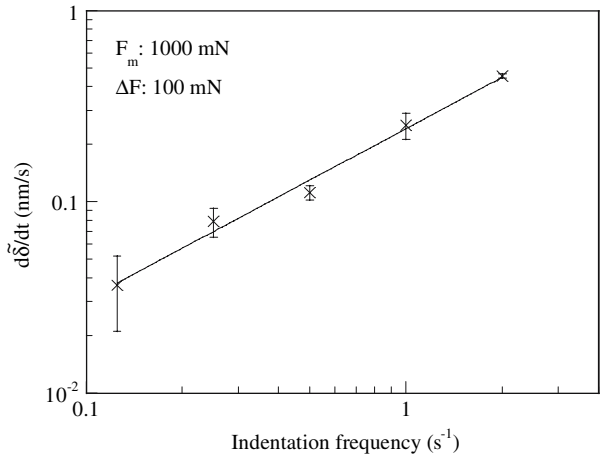

Fig. 12 Dependence of the steady state penetration speed on the indentation frequency for the mean load of 1,000 mN and the load amplitude of 100 mN—suggesting the likely quick emission of negative dislocation and faster interaction of dislocations

the approach used in the analysis of fatigue crack propagation [19], one can assume a power law relation between the steady state penetration speed and the indentation frequency as

$$\mathrm{d}\tilde{\delta}(t)/\mathrm{d}t = C_3 f^{n_6} \tag{11}$$

where C_3 is a constant and n_6 is an index. From Fig. 12, one obtains n_6 of 1. The steady state penetration speed is proportional to the indentation frequency.

The dependence of the average plastic energy dissipated per cycle on the indentation frequency is shown in Fig. 13. The average plastic energy dissipated per cycle increases with increasing indentation fre-

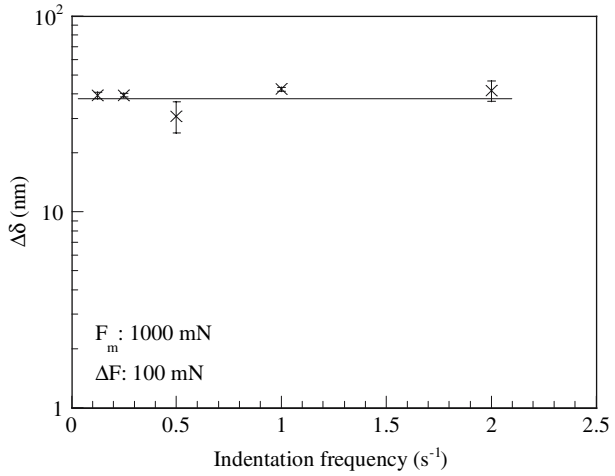

Fig. 11 Dependence of the amplitude of the indentation depth on the indentation frequency for the mean load of 1,000 mN and the load amplitude of 100 mN

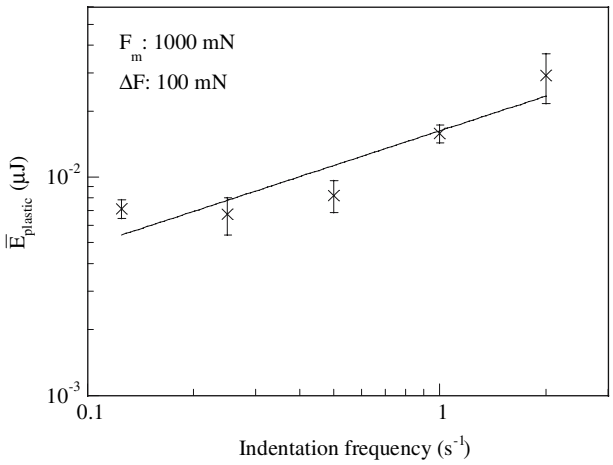

Fig. 13 Dependence of the average plastic energy dissipated per cycle on the indentation frequency for the mean load of 1,000 mN and the load amplitude of 100 mN

quency. Due to the work-softening of Al under the action of higher indentation frequency, more plastic flow is created and higher plastic energy is dissipated in each indentation cycle. Assuming a power law relation between the average plastic energy dissipated per cycle and the indentation frequency as

$$\bar{E}_{\text{plastic}} = \alpha_3 f^{n_7} \tag{12}$$

where α_3 is a constant and n_7 is an index, one obtains n_7 of 0.53.

Conclusion

The dynamic plastic deformation of aluminum was studied at ambient temperature using the cyclic indentation technique. Differing from the quasi-static indentation, the indenter continuously penetrated into the material and reached a steady state at which the penetration speed was a constant. The dependences of the amplitude of the cyclic indentation depth, the penetration speed at the steady state and the average plastic energy dissipated per cycle on the cyclic indentation load were evaluated. Stable hysteresis loop of the indentation load-indentation depth was observed, and the plastic energy dissipated in each cycle appeared to be approximately constant. On the basis of the experimental results, the following conclusions can be drawn.

1. Under the experimental conditions, the amplitude of the cyclic indentation depth was basically controlled by the amplitude of the cyclic indentation load, independent of the mean indentation load and the indentation frequency.
2. The steady state penetration speed decreased with increasing the amplitude of the cyclic indentation load due to the formation of larger size in plastic zone when subjected to cyclic indentation load with larger load amplitude.
3. The steady state penetration speed decreased with the increase of the mean load—local strain hardening induced by the cyclic indentation load increases the resistance to the penetration of the indenter.
4. Higher indentation frequency likely leads to faster emission of negative dislocations during the unloading and causes strain-softening. This leads to the increase of the steady state penetration speed with the increase of the indentation frequency.
5. The average plastic energy dissipated per cycle increases with the amplitude of the cyclic indentation load due to the formation of large plastic zone underneath the indentation, while it decreases with the increase of the mean indentation load because of the strain hardening. The strain-softening introduced by higher indentation frequency reduces the resistance for the propagation of the plastic zone and dissipates more energy during each loading-unloading cycle.

Acknowledgments This research is supported by NSF through a grant CMS-0508989 and Kentucky Science and Engineering Foundation through a grant KSEF-148-502-03-73.

References

1. Klesnil M, Lukas P (1980) Fatigue of metallic materials. Amsterdam, The Netherlands7 Elsevier Science
2. Sarfarazi M, Ghosh K (1987) Eng Fract Mech 27:257
3. Samuels LE (1986) In: Blau PJ, Lawn BR (eds) Microindentation techniques in materials science and engineering, ASTM STP 889. Am. Soc. Testing and Mater., Philadelphia, pp 5–25
4. Yang FQ, Jiang CB, Du WW, Zhang ZQ, Li SX, Mao SX (2005) Nanotechnology 16:1073
5. Vaughan DAJ, Guiu F (1887) Brit Ceram Proc 39:101
6. Reece M, Guiu F (1991) J Am Ceram Soc 74:148
7. Takakura E, Horibe S (1992) J Mater Sci 27:6151
8. Guillou M-O, Henshall JL, Hooper RM (1993) J Am Ceram Soc 76:1832
9. Henshall JL, Guillou M-O, Hooper RM (1996) Fatigue Fract Eng Mater Struct 19:903
10. Guiberteau F, Padture NP, Cai H, Lawn BR (1993) Phil Mag A 68:1003
11. Cai H, Kalceff MAS, Hooks BM, Lawn BR, Chyung K (1994) J Mater Res 9:2654
12. Padture NP, Lawn BR (1995) J Am Ceram Soc 78:1431
13. Kim DK, Jung Y-G, Peterson 1M, Lawn BR (1999) Acta Mater 42:4711
14. Ann L (1999) J Am Ceram Soc 82:178
15. Li JCM, Chu SNG (1979) Scripta Metall 13:1021
16. Chu SNG, Li JCM (1980) J Eng Mater Tech Trans ASME 102:337
17. Loubet JL, Georges JM, Meille G (1986) In: Blau PJ, Lawn BR (eds) Vickers indentation curves of elastoplastic materials, ASTM STP 889. Am. Soc. Testing and Mater., Philadelphia, pp 72–89
18. Sneddon IN (1992) Quart J Mech Appl Math 45:607
19. Suresh S (1998) Fatigue of materials, 2nd edn. Cambridge University Press
20. Cheng YT, Cheng CM (2004) Mater Sci Eng R44:91
21. Yang FQ, Peng LL, Okazaki K (2004) Metal Mater Trans A 35:3323
22. Hill R (1950) The mathematical theory of plasticity. Clarendon Press, Oxford
23. Johnson KL (1970) J Mech Phys Solids 18:115
24. Yang FQ, Peng LL, Okazaki K (2004) J Mater Res 19:1243